

Eccentric Dynamical Tides

Yubo Su¹, Dong Lai¹

¹ *Cornell Center for Astrophysics and Planetary Science, Department of Astronomy, Cornell University, Ithaca, NY 14853, USA*

Accepted XXX. Received YYY; in original form ZZZ

ABSTRACT

Abstract

Key words: keywords

1 INTRODUCTION

This problem is important.

2 THEORY

The primary goal of the paper is to evaluate [Equation 8](#), the total torque on a star due to dynamical tides excited by an eccentric perturber. We assume all frequencies excite outgoing waves (no standing modes) to simplify, and our results are generally most applicable for larger eccentricities $e \gtrsim 0.5$.

The primary results of the paper are [Equation 20](#) and [Equation 22](#), which are shown in [Figure 3](#), [Figure 4](#), and [Figure 5](#) to be reasonably accurate across a range of spins and eccentricities. The energy dissipation rate is also computed using similar techniques and show good agreement (see [Figure 6](#) and [Figure 7](#)).

2.1 Summary of Existing Work

Consider a star subject to the perturbing potential of a perturbing star with mass M_2 . For a general eccentric orbit, the potential to quadrupolar order can be decomposed into a sum over circular

orbits (Vick et al. 2017; Storch & Lai 2013):

$$U = \sum_m U_{2m}(\vec{r}, t), \quad (1)$$

$$U_{2m}(\vec{r}) = -\frac{GM_2 W_{2m} r^2}{D(t)^3} e^{-imf(t)} Y_{2m}(\theta, \phi), \quad (2)$$

$$= -\frac{GM_2 W_{2m} r^2}{a^3} Y_{2m}(\theta, \phi) \sum_{N=-\infty}^{\infty} F_{Nm} e^{-iN\Omega t}, \quad (3)$$

$$F_{Nm} = \frac{1}{\pi} \int_0^\pi \frac{\cos[N(E - e \sin E) - mf(E)]}{(1 - e \cos E)^2} dE. \quad (4)$$

We denote $W_{2\pm 2} = \sqrt{3\pi/10}$, $W_{2\pm 1} = 0$, $W_{20} = -\sqrt{\pi/5}$, $D(t)$ the instantaneous distance between the star and perturber, $f(t)$ the true anomaly, Y_{lm} the spherical harmonics, and Ω the mean motion of the companion. Note that F_{Nm} are the *Hansen coefficients* for $l = 2$. The total torque on the star is known (Vick et al. 2017):

$$\tau = \sum_{N=-\infty}^{\infty} F_{N2}^2 \tau_N, \quad (5)$$

where τ_N is the torque exerted by any particular N mode on the star.

For a circular orbit at fixed semimajor axis a , the torque exerted on the star by the companion is given by Kushnir et al. 2017:

$$\tau = \hat{T}(r_c, \omega) \operatorname{sgn}\left(1 - \frac{2\Omega_s}{\omega}\right) \left|1 - \frac{2\Omega_s}{\omega}\right|^{8/3}, \quad (6)$$

$$\hat{T}(r_c, \omega) \equiv \frac{GM_2 r_c^5}{a^6} \left(\frac{\omega}{\sqrt{GM_c/r_c}}\right)^{-8/3} \left[\frac{r_c}{g_c} \left(\frac{dN^2}{d \ln r}\right)_{r=r_c}\right]^{-1/3} \frac{\rho_c}{\bar{\rho}_c} \left(1 - \frac{\rho_c}{\bar{\rho}_c}\right)^2 \left[\frac{3}{2} \frac{3^{2/3} \Gamma^2(1/3)}{5 \cdot 6^{4/3}} \frac{3}{4\pi} \alpha^2\right], \quad (7)$$

where $1 - \frac{2\Omega_s}{\omega}$ is the dimensionless pattern frequency of a companion with orbital frequency ω , and $\alpha \simeq 1$ is defined in Equation A32 of Kushnir et al. 2017. Further notation includes: r_c the radius of the core, M_c the mass of the core, g_c the gravitational acceleration at the radiative-convective boundary (RCB), N^2 the Brunt-Vaisala frequency, r radial coordinate within the star, ρ_c the density at the RCB, and $\bar{\rho}_c$ the average density of the convective core.

Plugging this into Equation 5 gives total torque

$$\tau = \hat{T}(r_c, \Omega) \sum_{N=-\infty}^{\infty} F_{N2}^2 \operatorname{sgn}\left(N - 2\frac{\Omega_s}{\Omega}\right) \left|N - 2\frac{\Omega_s}{\Omega}\right|^{8/3}. \quad (8)$$

We next aim to express Equation 8 in simple closed form.

2.2 $m = 2$ Hansen Coefficient Behavior at High Eccentricity

Recall that the Hansen coefficients are defined as the Fourier series coefficients of part of the disturbing function

$$\frac{a^3}{D(t)^3} e^{-imf} = \sum_{N=-\infty}^{\infty} F_{Nm} e^{-iN\Omega t}. \quad (9)$$

Observe that $F_{-Nm} = F_{N-m}$. We further observe the following facts about the Hansen coefficients F_{N2} :

- For substantial eccentricities, F_{N2} has only one substantial peak. Defining

$$N_{\text{peri}} \equiv \frac{\Omega_p}{\Omega}. \quad (10)$$

where $\frac{\Omega_p}{\Omega} \equiv \frac{\sqrt{1+e}}{(1-e)^{3/2}}$, is the orbital frequency at pericenter, we find the peak of F_{N2} occurs at $\approx \sqrt{2}N_{\text{peri}}$ (see [Figure 1](#)). In fact, for $N < 0$, $F_{N2} \approx 0$ to good accuracy.

- We seek an analytically tractable formula for the Hansen coefficients. We guess form

$$F_{N2} \approx cN^p e^{-N/\eta}. \quad (11)$$

Two primary considerations enter into this fitting law: (i) since the left hand side of [Equation 9](#) is smooth in time, the Fourier coefficients must have an exponential tail; (ii) since there are no characteristic timescales between Ω and Ω_p , we anticipate the Hansen coefficients must be scale free between $N = 1$ and $N \sim \Omega_p/\Omega$, i.e. a power law.

- Empirically, we find that [Equation 11](#) is quite accurate for $e \gtrsim 0.5$, such that $N_{\text{max}} \gg 1$. Furthermore, we find that $p \approx 2$ is roughly independent of e .

Analytical manipulation shows that $\arg\max_N F_{N2} = p\eta$, and therefore

$$\eta \approx \frac{N_{\text{max}}}{p} \approx \frac{N_{\text{peri}}}{\sqrt{2}}. \quad (12)$$

Finally, we can lastly constrain c as well. Consider Parseval's theorem applied to [Equation 9](#)

$$\frac{1}{T} \int_0^T \left| \frac{a^3}{D(t)^3} e^{-imf} \right|^2 dt = \sum_{N=-\infty}^{\infty} |F_{Nm}|^2. \quad (13)$$

The left hand side can be integrated in closed form

$$\frac{1}{T} \int_0^T \left| \frac{a^3}{D(t)^3} e^{-imf} \right|^2 dt = \frac{1}{(1-e^2)^{9/2}} \left[1 + 3e^2 + \frac{3e^4}{8} \right]. \quad (14)$$

For sufficiently large e the right hand side does not change too drastically from term to term

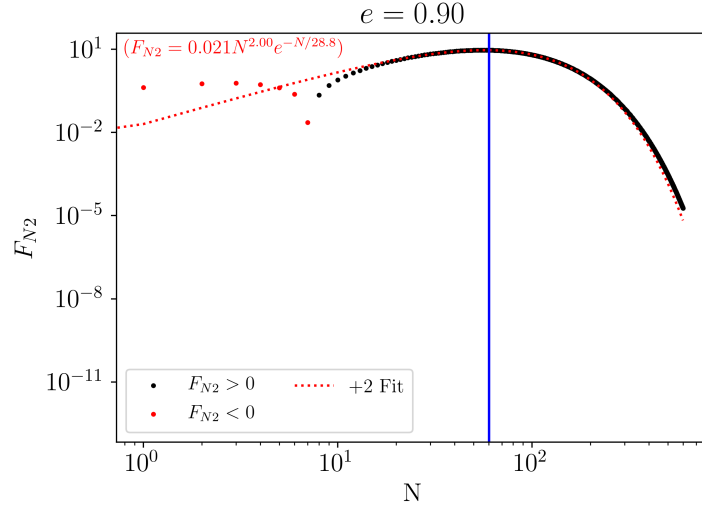


Figure 1. Plot of Hansen coefficients F_{N2} for $N > 0$, where red dots denote negative values. The red dashed line is the fitted function of form Equation 11 with the fit values overlaid in red text. Also shown in the blue vertical line is the location of N_{peri} .

($N_{\text{max}} \gg 1$), we can approximate

$$\sum_{N=-\infty}^{\infty} |F_{Nm}|^2 \approx \sum_{N=1}^{\infty} C^2 N^{2p} e^{-2N/\eta}, \quad (15)$$

$$\approx \int_0^{\infty} C^2 N^{2p} e^{-2N/\eta} dN, \quad (16)$$

$$= C^2 \left(\frac{\eta}{2}\right)^{2p+1} \Gamma(2p+1). \quad (17)$$

Thus, we constrain C as well

$$C \approx \sqrt{\frac{1 + 3e^2 + \frac{3e^4}{8}}{(1 - e^2)^{9/2}} \frac{1}{\left(\frac{\eta}{2}\right)^{2p+1} \Gamma(2p+1)}}. \quad (18)$$

The agreement of this fit of the Hansen coefficients as well as the accuracy (C, p, η) parameterization as a function of e can be seen in Figure 1 and Figure 2 respectively. Note that at moderate eccentricities $e \lesssim 0.7$, p is very poorly constrained, since it is dominant only in the regime $N \lesssim N_{\text{max}}$, which has fewer values for smaller eccentricities. Thus, we fixed $p = 2$ from our high-eccentricity fits ($e \gtrsim 0.9$) and assumed it is universal. We found indeed this does not significantly worsen fits at moderate eccentricities.

2.3 Closed Form for Torque

Given this, we can return to Equation 8 and evaluate the sum using the above parameterization. Again, for sufficiently large eccentricities that $N_{\text{max}} \gg 1$, we can convert the sum to an integral. There are then two primary regimes (we take $p = 2$):

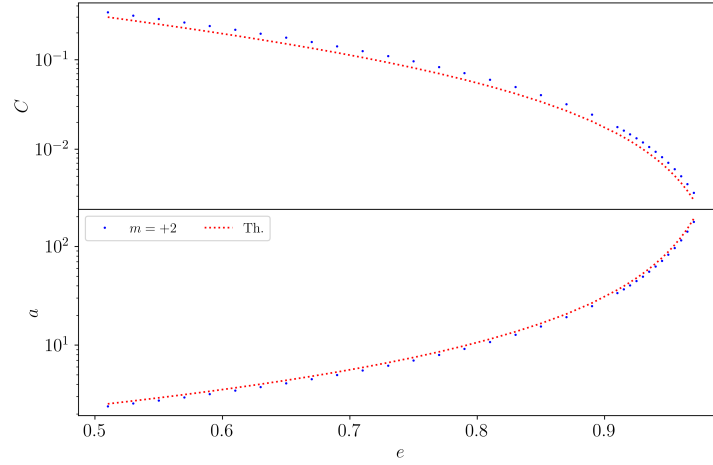


Figure 2. Plot of C , η as a function of e . Blue dots indicate the numerical fit to F_{N2} for $N > 0$ while red dashed lines reflect the predictions of Equation 12 and Equation 18 respectively. Note that $p = 2$ is taken to be fixed in the numerical fit.

- Let $\Omega_s/\Omega \ll N_{\text{peri}}$, then the sign term is just the sign of N , and $\left| \pm N - \frac{2\Omega_s}{\Omega} \right| \sim |N| \left(1 - \frac{\Omega_s/\Omega}{N_{\text{peri}}} \right)$. Note that while isn't the obvious expansion, the torque changes sign at $N \approx N_{\text{peri}}$ so this is the most natural choice for the leading order correction for Ω_s and seems to work well. This gives

$$\tau \approx \hat{T}(r_c, \Omega) \left(1 - \frac{\Omega_s/\Omega}{N_{\text{peri}}} \right)^{8/3} \left[C^2 \int_0^\infty N^{2p+8/3} e^{-2N/\eta} dN \right], \quad (19)$$

$$\approx \hat{T}(r_c, \Omega) \left[C^2 \left(\frac{\eta}{2} \right)^{23/3} \Gamma \left(\frac{23}{3} \right) \right]. \quad (20)$$

- Alternatively, let $\Omega_s/\Omega \gg N_{\text{peri}}$, then the sign is just always negative and $\left| N - \frac{2\Omega_s}{\Omega} \right| \sim \frac{2\Omega_s}{\Omega} - N_{\text{max}}$, and we find

$$\tau \approx -\hat{T}(r_c, \Omega) \left(\frac{2\Omega_s}{\Omega} - N_{\text{max}} \right)^{8/3} \left[C^2 \int_0^\infty N^{2p} e^{-2N/\eta} dN \right], \quad (21)$$

$$\approx -\hat{T}(r_c, \Omega) \left(\frac{2\Omega_s}{\Omega} - N_{\text{max}} \right)^{8/3} \left[C^2 \left(\frac{\eta}{2} \right)^5 \Gamma(5) \right]. \quad (22)$$

The existence of a pseudo-synchronized state at $\Omega_s \sim N_{\text{peri}}\Omega$ is already evident, as the sign of the torque changes in the two regimes. We showcase three plots showing the accuracy of this piecewise description of $\tau(e, \Omega_s/\Omega)$, Figure 3, Figure 4, Figure 5.:

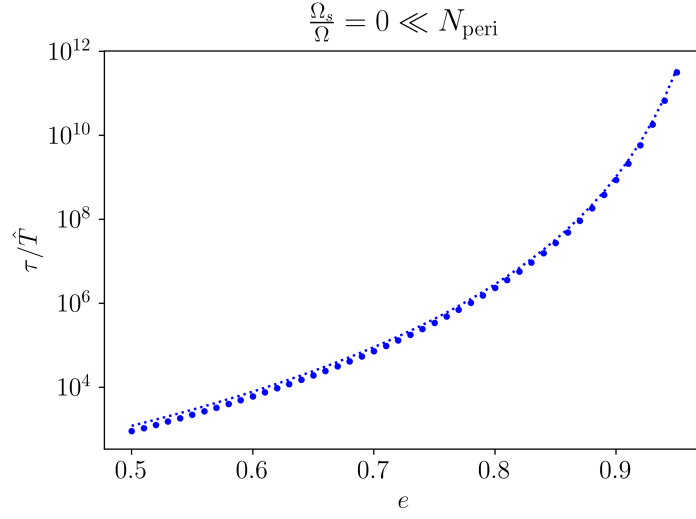


Figure 3. Tidal torque on a slowly spinning star with a companion having orbital eccentricity e . Blue dots represent explicit summation of Equation 8, while the blue dashed line is Equation 20.

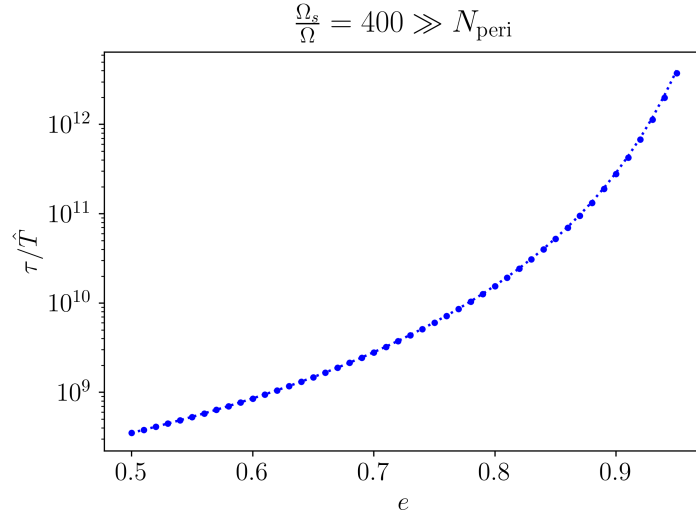


Figure 4. Tidal torque on a rapidly spinning star with a companion having orbital eccentricity e . Blue dots represent explicit summation of Equation 8, while the blue dashed line is Equation 22.

2.4 Closed Form for Heating

Energy transfer into the star due to this torque (including the $m = 0$ component) in the inertial frame is given by Vick et al. 2017:

$$\dot{E}_{\text{in}} = \frac{1}{2} \hat{T}(r_c, \Omega) \sum_{N=-\infty}^{\infty} \left[N \Omega F_{N2}^2 \text{sgn}(\sigma) |\sigma|^{8/3} + \left(\frac{W_{20}}{W_{22}} \right)^2 \Omega F_{N0}^2 |N|^{11/3} \right]. \quad (23)$$

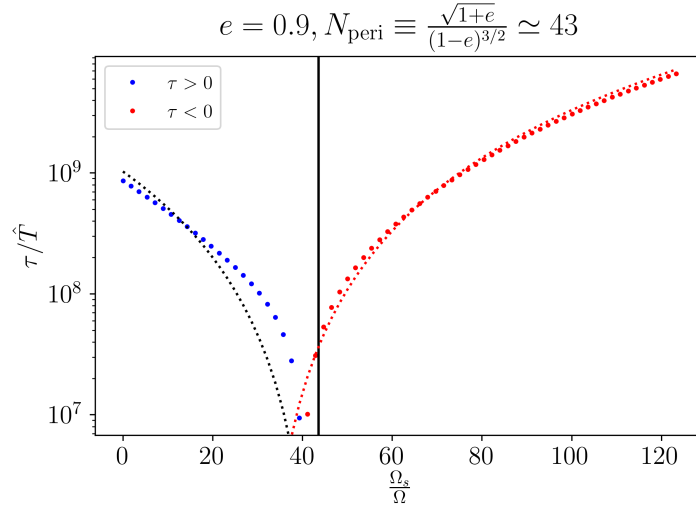


Figure 5. Tidal torque as a function of spin for a highly eccentric $e = 0.9$ companion. Blue dots represent explicit summation of Equation 8, while the blue dashed line is the piecewise prediction of Equation 20 and Equation 22 together. The vertical black line is the analytical $N_{\text{peri}} = 43$. While the pseudo-synchronization frequency differs somewhat from N_{peri} and the prediction of the piecewise torque, the qualitative behavior is very well captured.

The $m = 2$ contribution can be analyzed similarly to the previous section, with an extra power of N ; we obtain

$$\dot{E}_{\text{in}}^{(m=2)} = \begin{cases} \frac{\hat{T}\Omega}{2} C^2 \left(\frac{\eta}{2}\right)^{26/3} \Gamma(26/3) & \frac{\Omega_s}{\Omega} \lesssim N_{\text{peri}}, \\ \frac{\hat{T}\Omega}{2} C^2 \left(\frac{2\Omega_s}{\Omega} - N_{\text{max}}\right)^{8/3} (\eta/2)^6 \Gamma(6) & \frac{\Omega_s}{\Omega} \gtrsim N_{\text{peri}}. \end{cases} \quad (24)$$

The $m = 0$ contribution involves a sum over F_{N0} . Since these coefficients are symmetric about a maximum at $N = 0$ and represent the Fourier series of a smooth function, we expect again an exponential tail. Empirically, we find

$$F_{N0} \propto e^{-\frac{|N|}{N_{\text{peri}}}\sqrt{2}}, \quad (25)$$

to be a robust parameterization. To fix normalization constant A , we again invoke Parseval's theorem as was done in Equation 13:

$$\frac{1 + 3e^2 + \frac{3e^4}{8}}{(1 - e^2)^{9/2}} \approx 2 \int_0^\infty A^2 e^{-\frac{N2\sqrt{2}}{N_{\text{peri}}}} dN, \quad (26)$$

$$\approx 2A^2 N_{\text{peri}} \sqrt{2}, \quad (27)$$

$$A = \sqrt{\frac{1 + 3e^2 + \frac{3e^4}{8}}{(1 - e^2)^{9/2}} \frac{1}{2N_{\text{peri}} \sqrt{2}}}. \quad (28)$$

With this, we easily obtain the contribution of the $m = 2$ heating terms using similar techniques

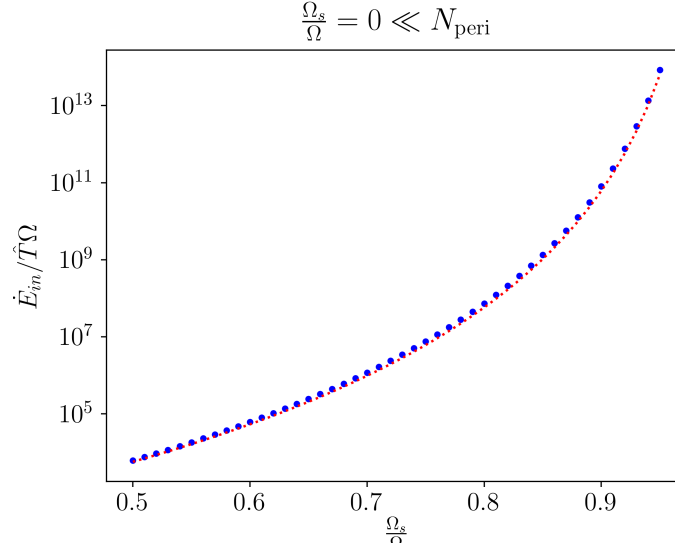


Figure 6. Plot of \dot{E}_{in} for a slowly spinning star. Blue points denote explicit summation of Equation 23 and the red dotted line represents the closed form Equation 31.

to before

$$\dot{E}_{in}^{(m=0)} = \hat{T}\Omega \left(\frac{W_{20}}{W_{22}} \right)^2 \int_0^\infty A^2 e^{-\frac{N}{N_{peri}} 2\sqrt{2}} N^{11/3} dN, \quad (29)$$

$$= \hat{T}\Omega \left(\frac{W_{20}}{W_{22}} \right)^2 A^2 \left(\frac{N_{peri}}{2\sqrt{2}} \right)^{14/3} \Gamma(14/3). \quad (30)$$

The total heating is just

$$\dot{E}_{in} = \dot{E}_{in}^{(m=2)} + \dot{E}_{in}^{(m=0)}. \quad (31)$$

We make plots in the two Ω_s regimes as a function of eccentricity in Figure 6 and Figure 7. Agreement is good again.

REFERENCES

- Kushnir D., Zaldarriaga M., Kollmeier J. A., Waldman R., 2017, Monthly Notices of the Royal Astronomical Society, 467, 2146
 Storch N. I., Lai D., 2013, Monthly Notices of the Royal Astronomical Society, 438, 1526
 Vick M., Lai D., Fuller J., 2017, Monthly Notices of the Royal Astronomical Society, 468, 2296

This paper has been typeset from a \LaTeX file prepared by the author.

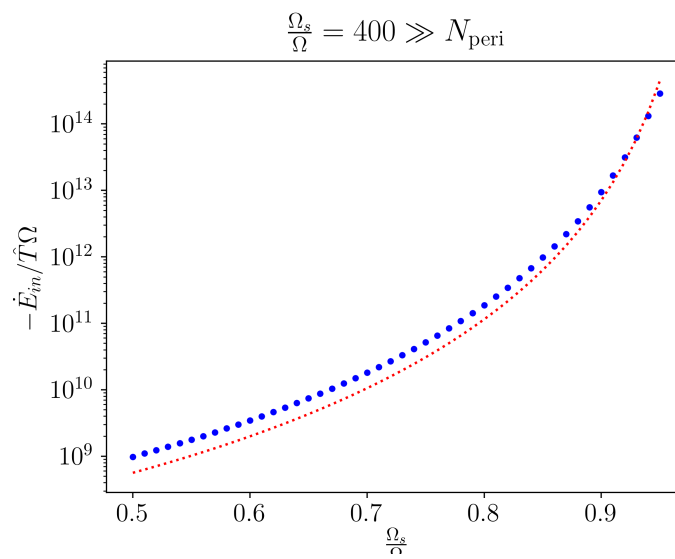


Figure 7. Same as Figure 6 but for a rapidly spinning star.